Author Manuscript

Author Manuscript

Author Manuscript

Author Manuscript

HHS Public Access

Author manuscript

Angew Chem Int Ed Engl. Author manuscript; available in PMC 2015 December 07.

Published in final edited form as:

Angew Chem Int Ed Engl. 2010 July 12; 49(30): 5076–5080. doi:10.1002/anie.201000265.

Programmable Shape-Shifting Micelles**

Miao-Ping Chien, **Anthony M. Rush**, **Matthew P. Thompson**, and **Nathan C. Gianneschi**

Department of Chemistry & Biochemistry, University of California, San Diego, 9500 Gilman Drive, MC 0343, La Jolla, CA 92093 (USA)

Nathan C. Gianneschi: ngianneschi@ucsd.edu

Keywords

aggregation; amphiphiles; block copolymers; DNA; micelles

Nanoscale particles that undergo reversible and defined changes in morphology in response to stimuli are expected to have broad utility in a range of applications, including targeted drug delivery, detection strategies, soft templates, and self-healing materials. To date, programmable materials with these properties have not been reported, despite the many elegant examples of stimuli-responsive soft nanoparticles and micelles.[1–11] Inspired by the utility of DNA as an informational molecule in nanotechnology,[12–20] we report herein DNA-encoded polymeric materials that are capable of in situ controlled, selective, reversible, and user-defined shifts in morphology. The design is based on polymeric micelles formed from a novel set of amphiphilic DNA-brush copolymers (Figure 1).[16,21] By utilizing the sequence-selective recognition properties of DNA,[22] and its performance as a substrate for selective enzymatic cleavage,[23,24] information stored in the micelle shell may be read and manipulated in several modes, causing dramatic changes in morphology and particle size.

The design rationale for DNA-programmed micelle morphology is based on rules that govern the aggregation of amphiphilic block copolymers.[25,26] Briefly, the phase (shape, size, overall morphology) of assembled amphiphiles is controlled by their geometric structure and electrostatics.[27] Therefore, it was hypothesized that DNA-brush copolymer amphiphiles would assemble into micelles with morphologies that are governed by sequence-selective interactions, which allow manipulation of the magnitude of steric and electrostatic repulsions in the micelle shells. Changes in geometric structure of the amphiphile are shown in Figure 1; larger cone angles give higher surface curvature aggregates (i.e., spheres). To demonstrate the concept of DNA-programmed micelle phase

**We gratefully acknowledge the support of this work by the University of California and from a Henry and Camille Dreyfus Foundation New Faculty Award to N.C.G. We wish to thank Mahealani R. Bautista and Lila K. Habib for their technical assistance, and Norm Olson for his generous assistance. We acknowledge use of the UCSD Cryo-Electron Microscopy Facility, which is supported in part by NIH grant 1S10 RR020016, a gift from the Agouron Institute, UCSD funds provided to Dr. Timothy S. Baker, the Nano-3 facilities at UCSD for use of their AFM instrument, the National Center for Microscopy and Imaging Research at San Diego supported by NIH, and the support of the National Science Foundation under CHE-0741968.

Correspondence to: Nathan C. Gianneschi, ngianneschi@ucsd.edu.

Supporting information for this article is available on the WWW.under http://dx.doi.org/10.1002/anie.201000265.

Author Manuscript Author Manuscript Author Manuscript Author Manuscript

transition, three types of sequence-selective interactions were chosen: 1) enzymatic cleavage, 2) isothermal hybridization of complementary single-stranded DNA (ssDNA), and 3) thermal melting and annealing of DNA duplexes.

The DNA-brush copolymer amphiphiles assemble into spherical micelles (Figure 1, blue spheres) approximately 25 nm in diameter, as characterized by transmission electron microscopy (TEM), atomic force microscopy (AFM), and dynamic light scattering (DLS; see Figure 1S in the Supporting Information for DLS and AFM studies). The DNA-brush copolymer amphiphiles contain a RNA base (rA) as an enzymatic cleavage site, two 18-membered ethylene glycol moieties that increase steric bulk of the hydrophilic block, and a fluorescein tag to allow monitoring of reactions that occur at the particle shell. To facilitate a sphere-to-cylinder phase transition, the spherical micelles were mixed with a DNA-based phosphodiesterase (DNAzyme[24]), which was conveniently synthesized to recognize a given DNA sequence and cut at a RNA base. This process resulted in complete, rapid catalytic turnover of the DNA substrate that formed the bulk of the hydrophilic block and generated a truncated ssDNA sequence. A subsequent sphere-to-cylinder phase transition occurs as the “new” surfactants reorganize and pack accordingly (see Figure 2S in the Supporting Information for data showing turnover of shell DNA). To facilitate a cylinder-to-sphere phase transition, a 19-base input DNA sequence ($\mathbf{In}_1$) was added. This sequence was designed to form a 9-base duplex with the truncated DNA in the cylinder shell. Subsequent cylinder-to-sphere transition occurs as the bulky, extended duplex is better accommodated in the spherical micelle phase. Therefore, the new structures (Figure 1, green spheres) contain a noncovalent DNA duplex that is amenable to sphere-to-cylinder phase transition utilizing DNA strand invasion.[28,29] This was achieved by addition of a perfectly complementary 19-base ssDNA ($\mathbf{In}_2$) designed to invade into the shorter 9-base duplex in the micelle shell. The more thermodynamically stable 19-base long duplex ($\mathbf{In}_1 \cdot \mathbf{In}_2$) departs, leaving the truncated ssDNA amphiphile to reassemble into the cylindrical phase.

The reversibility of the phase transitions was examined in solution by DLS (Figure 2), with a confirmation of morphologies by TEM (Figure 3S in the Supporting Information). DLS data for isothermal DNA-directed phase transitions are shown as the percentage (volume distribution) of particles at the 396 nm size class, which result from various input additions after two-hour incubation periods (Figure 2). Initially, solutions of the spherical particles showed no observable scattering intensity for aggregates above 30 nm. Indeed, the particle diameter (reported as the hydrodynamic diameter D_h) was constant in the absence of DNAzyme over a time scale of many weeks. However, mixing of the spherical particles with the DNAzyme for two hours caused the expected increase in the D_h value (Figure 2a). Next, this solution was mixed with $\mathbf{In}_1$ showing the expected contraction in D_h. Subsequent addition of $\mathbf{In}_2$ results in duplex $\mathbf{In}_1 \cdot \mathbf{In}_2$, regenerating the truncated shell structure and causing another expansion of particle size. To complete the isothermal cycle, the particles were again treated with $\mathbf{In}_1$ resulting in regeneration of small aggregates. In addition, this isothermal phase-cycling process was monitored by the uptake and release of a small-molecule dye (Figure 4S in the Supporting Information).

The hybridization state of complementary oligonucleotides is disrupted at elevated temperatures. The isothermal cycling experiments (Figure 2a) show a dependence of the

Author Manuscript Author Manuscript Author Manuscript Author Manuscript

morphology on the hybridization state of the DNA. Similarly, cycling of the solution temperature resulted in aggregate size changes, which were dependent on whether or not the DNA in the amphiphile was in duplex or single-stranded form (Figure 2b). These data show a correlation between the temperature of the solution and the aggregate size in solution, that is, the size increases above the melting temperature of the DNA duplex and decreases below the melting temperature. These data complement the isothermal cycling experiment with the same correlation with respect to the hybridization state of the amphiphile.

To further elucidate the mechanism and assess the selectivity of the DNAzyme-directed phase transition, the process was examined by TEM and DLS (Figure 3), and studied by fluorescence microscopy (Figure 4). TEM and DLS data show a solution populated with a decreasing concentration of intact 25 nm spheres (Figure 3, red curve) and growing cylindrical aggregates with time (Figure 3, blue curve; see also Figure 5S in the Supporting Information). The TEM data correlates with the increase in D_h observed by DLS (Figure 3, green curve). After one day, cylinders could be observed in high density, and TEM data showed the presence of well-defined cylinders (Figure 3d and inset). After two days in the presence of the DNAzyme, TEM data confirmed low concentrations of intact spherical structures (Figure 3e), and the presence of cylinders greater than 1 μm in length. This phase-transition process constitutes an approximate 100-fold increase in size and a dramatic change in morphology, which results in clear solutions and no precipitation. Insight into the mechanism of this process is provided by the observation that complete turnover of the shell DNA of the initial spheres is rapidly achieved (Figure 2S in the Supporting Information) prior to complete phase transition. Therefore, after DNAzyme addition, competing equilibria for monomeric amphiphile assembly are rapidly established and result in cylinder growth (amphiphile↔cylinder versus amphiphile↔sphere).

A series of fluorescence microscopy experiments were conducted to test if a mixed population of particles encoded with different DNA sequences could respond independently and selectively in the presence of competing DNAzymes. Two fluorescent particles that contain two different DNA sequences were synthesized; one labeled with a fluorescein dye (through a fluorescein–thymidine (FlrT) phosphoramidite) and the other labeled with a rhodamine dye (through a rhodamine–thymidine (RhT) phosphoramidite; Figure 4 and Figure 6S in the Supporting Information). Conveniently, micrometer-sized fibers (bundles of cylinders) could be imaged by light microscopy; 25 nm spheres, which were below the resolution limit, contributed to diffuse background fluorescence that had much lower intensity than the fibers. The red and green fluorescent particles were mixed together and treated with two different DNAzymes (D-1 and D-2), each of which was complementary to one of the dye-labeled particles. Introduction of the DNAzyme selective for the sequence within the green fluorescent particle shell (D-1) resulted in the formation of green fluorescent cylinders, with no observable red fluorescence (Figure 4b). Conversely, only red fluorescent particles reacted with the DNAzyme selective for the sequence within their shell (D-2). This selectivity is confirmed by the absence of green fluorescence in the images of these cylinder structures and the appearance of red fluorescent cylinders (Figure 4c). Finally, when mixed with D-1 and D-2, both spheres in the mixture reacted, which caused the formation of structures containing both red and green fluorophores (Figure 4d). These

Author Manuscript Author Manuscript Author Manuscript Author Manuscript

studies provide evidence supporting the conclusion that truncation of the DNA is a necessary requirement for phase transition and is indeed sequence-selective. This experiment is possible because the two amphiphiles are chemically similar except for the information encoded in their respective DNA sequences. This characteristic makes each particle type in the mixed population independently addressable, a feature that is not easily accessible for systems designed to respond to non-informational stimuli such as temperature, light, or pH.

In summary, we have demonstrated the utility of DNA as an informational tool for morphology control in discrete, stimuli-responsive, nanoscale polymeric materials.[13] It is expected that this approach will be amenable for extension to a variety of stimuli given the versatility of nucleic acids as molecules that are capable of multiple modes of selective recognition. In a broader context, the development of generally applicable methods for predictably controlling size, shape, and functionality of soft materials at the nano-meter length scale will be critical for realizing their tremendous potential.[30–39]

Supplementary Material

Refer to Web version on PubMed Central for supplementary material.

References

1. Wang Y, Xu H, Zhang X. Adv Mater. 2009; 21:2849.
2. Zhang L, Yu K, Eisenberg A. Science. 1996; 272:1777. [PubMed: 8662482]
3. Bütün V, Billingham NC, Armes SP. J Am Chem Soc. 1998; 120:11818.
4. LaRue I, Adam M, Pitsikalis M, Hadjichristidis N, Rubinstein M, Sheiko SS. Macromolecules. 2006; 39:309.
5. Liu X, Jiang M. Angew Chem. 2006; 118:3930.Chem Int Ed. 2006; 45:3846.
6. Ishihara Y, Bazzi HS, Toader V, Godin F, Sleiman HF. Chem Eur J. 2007; 13:4560. [PubMed: 17343289]
7. Kim JH, Lee S, Park K, Nam HY, Jang SY, Youn I, Kim K, Jeon H, Park RW, Kim IS, Choi K, Kwon IC. Angew Chem. 2007; 119:5881–5884.Chem Int Ed. 2007; 46:5779–5782.
8. Li Y, Du W, Sun G, Wooley KL. Macromolecules. 2008; 41:6605.
9. Roy D, Cambre JN, Sumerlin BS. Chem Commun. 2009:2106.
10. Fernyhough C, Ryan AJ, Battaglia G. Soft Matter. 2009; 5:1674.
11. Amir RJ, Zhong S, Pochan DJ, Hawker CJ. J Am Chem Soc. 2009; 131:13949. [PubMed: 19739628]
12. Seeman NC. Mol Biotechnol. 2007; 37:246. [PubMed: 17952671]
13. Aldaye FA, Palmer AL, Sleiman HF. Science. 2008; 321:1795. [PubMed: 18818351]
14. Gothelf KV, LaBean TH. Org Biomol Chem. 2005; 3:4023. [PubMed: 16267576]
15. Storhoff JJ, Mirkin CA. Chem Rev. 1999; 99:1849. [PubMed: 11849013]
16. Alemdaroglu FE, Herrmann A. Org Biomol Chem. 2007; 5:1311. [PubMed: 17464398]
17. He Y, Ye T, Su M, Zhang C, Ribbe AE, Jiang W, Mao C. Nature. 2008; 452:198. [PubMed: 18337818]
18. Ofir Y, Samanta B, Rotello VM. Chem Soc Rev. 2008; 37:1814. [PubMed: 18762831]
19. Venkataraman S, Dirks Robert M, Rothemund Paul WK, Winfree E, Pierce Niles A. Nat Nanotechnol. 2007; 2:490. [PubMed: 18654346]
20. Adleman LM. Science. 1994; 266:1021. [PubMed: 7973651]
21. Li Z, Zhang Y, Fullhart P, Mirkin CA. Nano Lett. 2004; 4:1055.

Author Manuscript Author Manuscript Author Manuscript Author Manuscript

22. Watson JD, Crick FH. Nature. 1953; 171:737. [PubMed: 13054692]
23. Kelly TJ Jr, Smith HO. J Mol Biol. 1970; 51:393. [PubMed: 5312501]
24. Santoro SW, Joyce GF. Proc Natl Acad Sci USA. 1997; 94:4262. [PubMed: 9113977]
25. Israelachvili JN, Mitchell DJ, Ninham BW. J Chem Soc Faraday Trans 2. 1976; 72:1525.
26. Jain S, Bates FS. Science. 2003; 300:460. [PubMed: 12702869]
27. Nagarajan R. Langmuir. 2002; 18:31.
28. Hazarika P, Ceyhan B, Niemeyer CM. Angew Chem. 2004; 116:6631.Angew Chem Int Ed. 2004; 43:6469.
29. Zhang DY, Winfree E. J Am Chem Soc. 2009; 131:17303. [PubMed: 19894722]
30. Smith D, Pentzer EB, Nguyen ST. Polym Rev. 2007; 47:419.
31. Geng Y, Dalhaimer P, Cai S, Tsai R, Tewari M, Minko T, Discher DE. Nat Nanotechnol. 2007; 2:249. [PubMed: 18654271]
32. Kishimura A, Koide A, Osada K, Yamasaki Y, Kataoka K. Angew Chem. 2007; 119:6197.Angew Chem Int Ed. 2007; 46:6085.
33. Kim KT, Cornelissen JJLM, Nolte RJM, van Hest JCM. Adv Mater. 2009; 21:2787.
34. Xia Y, Olsen BD, Kornfield JA, Grubbs RH. J Am Chem Soc. 2009; 131:18525. [PubMed: 19947607]
35. MacKay JA, Chen M, McDaniel JR, Liu E, Simnick AJ, Chilkoti A. Nat Mater. 2009; 8:993. [PubMed: 19898461]
36. Shah RN, Shah NA, Del Rosario Lim MM, Hsieh C, Nuber G, Stupp SI. Proc Natl Acad Sci USA. 2010; 107:3293. [PubMed: 20133666]
37. Peer D, Karp JM, Hong S, Farokhzad OC, Margalit R, Langer R. Nat Nanotechnol. 2007; 2:751. [PubMed: 18654426]
38. Haag R. Angew Chem. 2004; 116:280.Angew Chem Int Ed. 2004; 43:278.
39. Nayak S, Lyon LA. Angew Chem. 2005; 117:7862.Angew Chem Int Ed. 2005; 44:7686.

Author Manuscript Author Manuscript Author Manuscript Author Manuscript

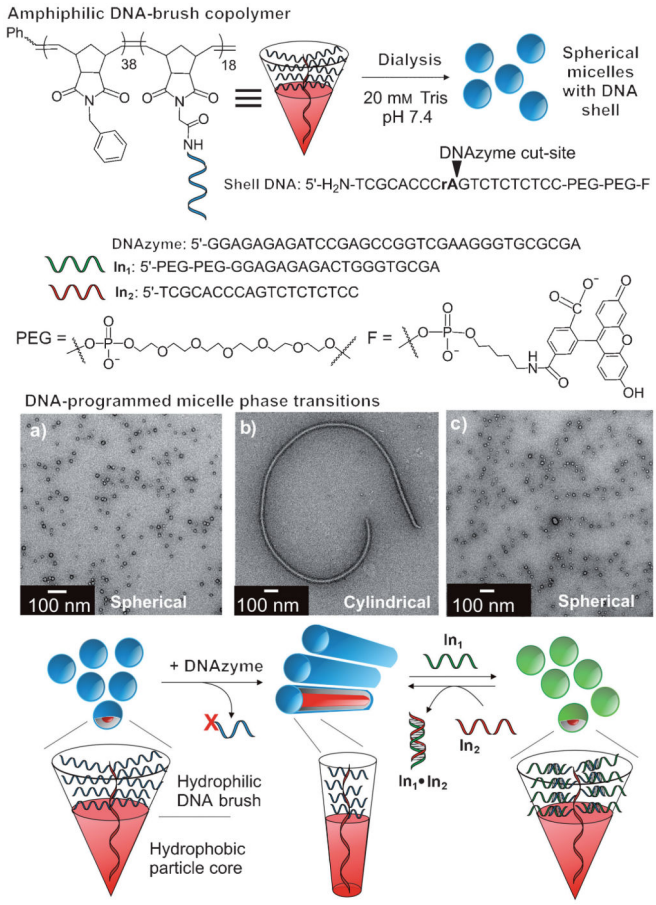

Figure 1.

Assembly of DNA-brush copolymers into micelles with spherical or cylindrical morphologies. Amphiphile structures are represented as cones for each respective morphology, with the hydrophobic domain highlighted in red. TEM images of a) 25 nm spherical micelles assembled from initial DNA-brush copolymers; b) cylindrical morphology formed following DNAzyme addition to spheres; c) spherical micelles (green) formed after addition of $\mathbf{In}_1$ to cylinders. See also Figure 3S in the Supporting Information.

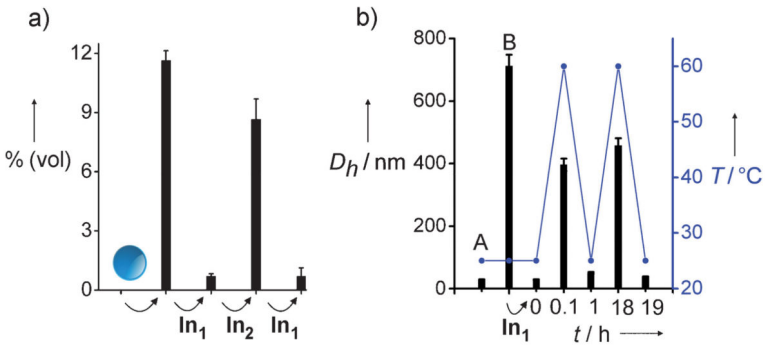

Figure 2.

Reversible phase cycling experiments. a) Isothermal hybridization and invasion. The y axis shows the percentage (volume distribution) of species in D_h = 396 nm size class versus input; measurements were obtained by DLS 2 h after each input addition beginning with 25 nm spheres. The D_h value of 396 nm was chosen as it is the largest aggregate size class observed by DLS at 2 h (see Figure 3). b) Variable-temperature DLS. Plot shows D_h of largest aggregates in solution at given time points. Initial spheres (A) were treated with DNAzyme for 18 hrs (B) prior to addition of $\mathbf{In}_1$. DLS measurement at t = 0 min taken 1 h after addition of $\mathbf{In}_1$. Ramp rate: 25→60°C in 5 min. Instrument cooling time was 60 min; sample was cooled by placing in ice bath for 5 min, then rested at RT for 55 min. Second heating cycle conducted 18 h later with same ramp rate (25→60°C in 5 min) and cooling time (60 min). Conditions: particles (0.14 g L^{-1}), DNAzyme (5 nm), $\mathbf{In}_1$ (50 nm), $\mathbf{In}_2$ (50 nm), 2-amino-2-hydroxymethyl-propane-1,3-diol (Tris; 20 mm, pH 7.4), $MgCl_2$ (50 mm).

Author Manuscript Author Manuscript Author Manuscript Author Manuscript

Author Manuscript Author Manuscript Author Manuscript Author Manuscript

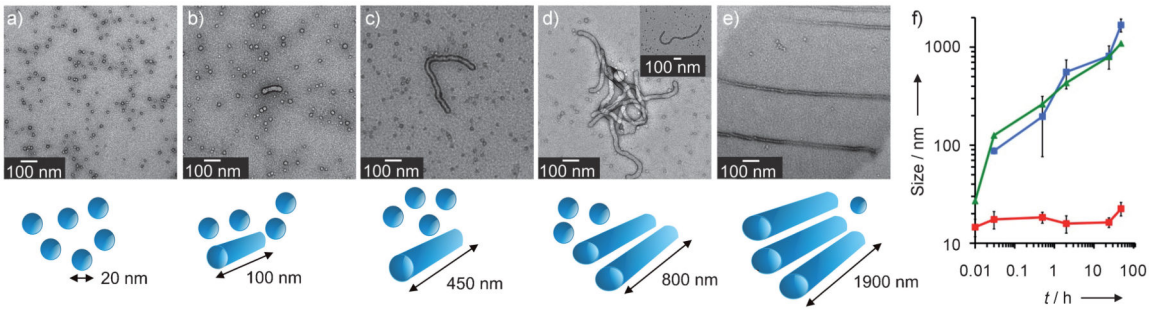

Figure 3.

DNA-directed size and phase change over time. Conditions: particles (0.14 g L^{-1}), Tris (20 mm, pH 7.4), $MgCl_2$ (50 mm). DNAzyme (5 nm) was mixed with particles at t = 0 min. a) t = 0 min, b) 2 min, c) 2 h, d) 1 day, e) 2 days. f) Particle size as a function of time following DNAzyme addition. Blue curve: average cylinder length (C_L) measured by TEM. Green curve: D_h value of largest aggregates measured by DLS. Red curve: Sphere diameter (S_D) measured by TEM. DLS data was taken at the time points shown following DNAzyme addition. Data points for C_L and S_D are averages of multiple measurements made from TEM images, with error bars indicating standard deviations (Figure 4S in the Supporting Information).

Author Manuscript Author Manuscript Author Manuscript Author Manuscript

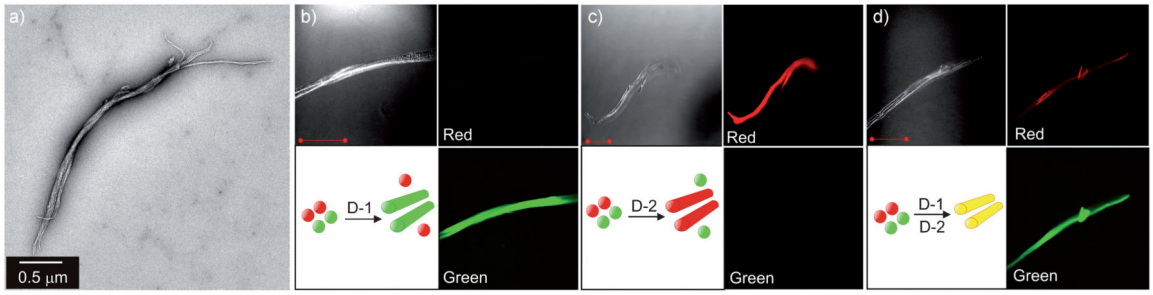

Figure 4.

Sequence-selective phase shifting observed by fluorescence microscopy. a) TEM image showing bundled cylinder structures analogous to optical images. Optical microscopy images show bright field, green and red fluorescence images taken after treatment with DNAzyme. b) D-1 recognizes only fluorescein labeled particles. c) D-2 recognizes only rhodamine labeled particles. d) D-1 and D-2 together cause fiber formation containing both labels. Optical image scale bars = 10 µm. Conditions: Micelles (0.14 g L^{-1}), DNAzyme (5 nm), Tris (20 mm, pH 7.4), $MgCl_2$ (50 mm). Shell DNA sequences are analogous to that shown in Figure 1, with an extra three bases at the 5′-terminus. The third base from the 5′-amide linkage to the polymer backbone is a dye-labeled thymidine residue (see the Supporting Information for DNA sequences used in these experiments).